Preprints of the 19th World Congress
The International Federation of Automatic Control
Cape Town, South Africa. August 24-29, 2014

Modelling Vehicle Body Structures for Active Buckling Control

James E. Trollope*. Keith J. Burnham*.

*Control Theory and Applications Centre (CTAC), Coventry University, Priory Street, Coventry CV1 5FB, UK
(Tel: 024-77-659196; e-mail: james.trollope@coventry.ac.uk).

Abstract: This paper introduces the concept of active buckling control and how it can be applied to vehicle body structures to improve safety. Active buckling control is achieved through the use of actively controlled materials, whereby the mechanical properties of a structure can be altered. The need for active buckling control is prompted by compatibility issues arising when vehicles of dissimilar mass collide. Effectively, the active buckling control system can stiffen the more vulnerable vehicle, as a result, sharing the collision energy more appropriately and improving the safety of the occupants. A model of a nonlinear force versus deformation characteristic is used within a simulation study to demonstrate the active buckling control concept; thereby reducing the undesirable energy distribution so that the collision energy is absorbed more appropriately.

Keywords: Active control, Automotive control, Bilinear models, Modelling, Piecewise linear, Least-squares approximation

1. INTRODUCTION

In recognition of the need for controlled absorption of kinetic energy arising from a collision of two (or more) vehicles, this paper addresses the concept of model-based active buckling control (ABC), hence modelling of the vehicle body structure (VBS). In a collision scenario the mechanical structure of a vehicle undergoes changes in stiffness as a function of the deformation of the load bearing members crumpling under axial compression. Crumple zones were first introduced in the design of the VBS in the late 1950s. Since its inception the basic idea has not significantly changed, with the crumple zones encouraged to passively deform via design; with weakened regions collapsing under pre-defined loads at certain locations.

More recently, since the late 1990s, vehicles on the roads in Europe are required to comply with EU safety standards and must meet criteria known as crashworthiness, with manufactures being legislated such that vehicles satisfy the European new car assessment programme (Euro NCAP) (Euro NCAP, 2013). The crashworthiness criteria include frontal impact, car to car side impact and pole side impact, with the objective being to test the energy absorption deformation properties of the VBS whilst resisting intrusion into the passenger compartment. The problem is further compounded by the well-known compatibility problem arising when two (or more) vehicles of differing mass collide, and the distribution of collision energy leads to an unacceptable level of aggressivity as experienced by the smaller vehicle.

An unfortunate side-effect of satisfying crashworthiness has been the steady increase in vehicle mass due to the need for crumple zones, with an average increase of 8kg per year being reported during 1980-2006 (Ellis, 2011). This trend is counter to the need to reduce CO_2 emissions and improve fuel efficiency, with reduction in the mass of VBS being desired. To simultaneously meet both crashworthiness and emission legislation there is an attendant need for radical change, thus prompting the need for actively controlled VBS, hence ABC.

In summary, combining the above requirements introduces the need for lightweight VBS that can adapt to various vehicle mass compatibility scenarios and actively absorb collision energy far more effectively than the current passive methods. Moreover, the need for ABC is heightened by the fact that the compatibility issue will be ever-present as smaller lightweight vehicles are introduced into the fleet.

1.1 Concept of active buckling control

This paper aims to both introduce and demonstrate the advantages of adopting an ABC concept, which is made feasible by the use of actively controlled materials (ACM) that have the property of actuating, hence achieving a mechanical structural change. Such an approach, combined with vehicle to vehicle (V2V) communication can be configured to provide a feedback loop, for a closed-loop active VBS. Consequently, it is anticipated that with the use of ACM, the mechanical properties of VBS can be altered based on exchanging data via V2V communication, effectively altering the buckling load, relating to the smallest positive eigenvalue, prior to an imminent collision. The smallest positive eigenvalue being the mode relating to the stiffness of the first collapsible member of the controlled VBS. The approach makes use of a multi-dimensional look-up table with an initial 'first guess' of the values of the buckling loads for each vehicle being further enhanced/refined using fuzzy logic interpolation and an on-board Kalman filtering approach for updating an estimate of

the predicted collision velocity (Trollope and Burnham, 2013a, b).

Adopting an approach as outlined above, it is expected that actively controlled VBS will lead naturally to lightweight structures, as crashworthiness will be achieved more efficiently. Moreover, when the compatibility problem is encountered, such scenarios will be dealt with more effectively, with collision energy being commensurably distributed amongst the colliding vehicles without compromising occupant protection.

2. COMPATIBILITY ISSUES

Section 1 briefly highlighted the compatibility issues that can affect the energy absorption performance of a structure, hence the safety of the occupants. This Section aims to highlight the fundamental limitations with the current Euro NCAP structural testing and how this might be improved by taking into account vehicles of differing mass.

2.1 Review of European NCAP

The Euro NCAP frontal impact test involves a vehicle being driven at 40mph (17.88m/s) with a 40% overlap into an immovable block with a deformable aluminium honeycomb face. Since the introduction of the Euro NCAP, the tests have proven successful, with reduced injuries and fatalities (Thatcham Insight, 2012). However, the underlying limitations with the test will now be highlighted. Firstly, Newton's third law states that all forces exist in equal and opposite pairs. Hence when a vehicle, denoted A, is subject to the Euro NCAP frontal impact test, colliding with an immovable block, denoted B, their respective forces, denoted $F_a = -F_b$ are created. Consequently, the test results achieved for one vehicle are comparable to vehicles of the same mass only. Furthermore, dissimilarities in vehicle stiffness and geometry may cause problems, effectively meaning that two vehicles of the same mass may not be compatible, e.g. one may have a stiffer passenger compartment and smaller crumple zones. Consequently, the passengers may experience different crash pulse characteristics (accelerations). For the purpose of simplicity, it is assumed here that vehicles have the same geometry.

2.1.1 Kinetic energy between two vehicles colliding

Consider the case of a frontal impact collision between two vehicles. Firstly the conservation of momentum will be considered, expressed as:

$$(m_a V_a + m_b V_b) = m_{a+b} V_f \tag{1}$$

where V_a and V_b are the vehicle velocities and V_f is the final velocity of the combined masses, respectively. Equation (1) implies that the two vehicle masses stay together after impact (perfectly plastic impact) and have the same velocity and displacement. The principle of conservation of energy states that the kinetic energy before and after a collision must be equal. This is expressed as follows:

$$\frac{1}{2}m_a V_a^2 + \frac{1}{2}m_b V_b^2 = \frac{1}{2}m_a V_f^2 + \frac{1}{2}m_b V_f^2 + \Delta E \tag{2}$$

where ΔE is the collision energy dissipated within the VBS.

2.1.2 Kinetic energy distribution

The ratio of energy absorption is proportional to the change in the velocities, denoted ΔV_a and ΔV_b, expressed as follows:

$$\Delta V_a = |V_f - V_a| \text{ and } \Delta V_b = |V_f - V_b| \tag{3}$$

where the following ratios can be deduced:

$$\Delta V_a : \Delta V_b \text{ is the same as } m_b : m_a, \tag{4}$$

so when $m_a = m_b$, $V_f = 0$ and the collision energy ΔE is distributed equally between the two colliding vehicles. However, when $m_a \neq m_b$ the collision absorbed by each vehicle, denoted E_a and E_b, is given, respectively, by:

$$E_a = \frac{m_b \Delta E}{(m_a + m_b)} \quad \text{and} \quad E_b = \frac{m_a \Delta E}{(m_a + m_b)} \tag{5}$$

thus reinforcing the vulnerability of the smaller vehicle, having to absorb the larger proportion of the energy.

2.1.3 Illustrative example

An example serves to illustrate the apportionment of collision energy. Consider Vehicle A of mass 1000kg and Vehicle B of mass 500kg. Vehicle A strikes stationary Vehicle B at 40mph (17.88m/s). The collision energy ΔE may be deduced to be $38.4kJ$, and, with the mass ratio being $2:1$ the ratio of $E_a : E_b$ is 1:2 so that the larger vehicle absorbs only $12.8kJ$ compared to $25.6kJ$ to be absorbed by the smaller vehicle.

Ideally the situation needs to be reversed, whereby the larger vehicle absorbs more of the collision energy, thereby reducing the aggressivity of the larger vehicle as perceived by the smaller. Essentially with ABC the smaller vehicle will actively stiffen more than the larger, with the latter 'cushioning' the smaller as more energy is absorbed.

2.2 Reduced aggressivity

Due to the compatibility issues highlighted in Section 2.1, it is anticipated that in the future, vehicles will be tested against vehicles of dissimilar masses. This introduces the need for reduced aggressivity, where the host vehicles are designed to take into account their own passengers and those of the partner vehicles, as opposed to the current situation, where the host vehicles are designed to take into account the host vehicle passengers only. This means that all vehicles will require ABC and the larger vehicles will need to be designed to have a greater capacity to absorb more energy than the smaller vehicles, with the latter being designed to have a greater capacity to stiffen.

The need for reduced aggressivity prompts the need for ABC of VBS in order to share more appropriately the energy absorption, so that the lightweight VBS stiffens dependent on

the mass of each vehicle, thereby reversing the undesirable scenario. This requires the structural properties to be actively modulated, leading to the proposed ABC scheme.

2.3 Actively controlled materials

Essentially, ACM may be exploited to bring about a desired change in the mechanical properties of structures. A feature of ACM is that they possess functions such as, sensing, actuating and controlling. ACM links mechanical engineering with control engineering, thus facilitating actively controlled structures with embedded functionality (Trollope and Burnham, 2013a, b). Examples of ACM include piezoelectric materials to change the stiffness i.e. Young's modulus and shape memory alloys to change the second moment of area. Piezoelectric materials have two properties; the direct and converse effect. When a mechanical force is applied to a piezoelectric material, a charge is created by the motion of the dipoles within the material. The reciprocal effect, applying an electric field, a mechanical response is achieved, typically a change in displacement. A shape memory alloy can undergo a shape change for a given electrical input or heat at a specific value.

3. ACTIVE BUCKLING CONTROL SYSTEM

This Section describes the basis of the ABC algorithm. A diagrammatic representation of the strategy is presented, taking into consideration the host vehicles ABC system only (Fig. 1).

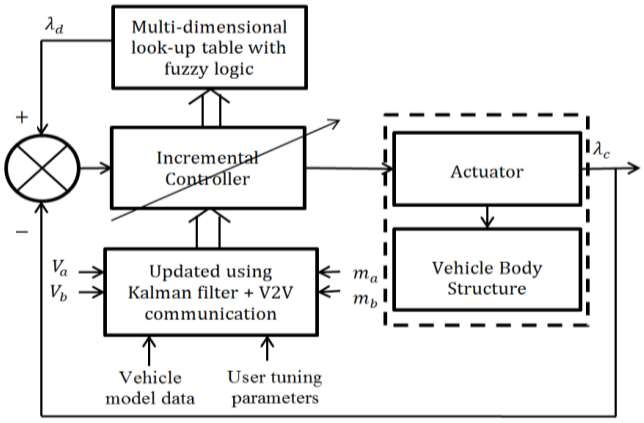

Fig. 1. ABC System for VBS with ACM

Once the advanced driver assistance systems (ADAS) have exhausted their collision mitigation functionalities and an imminent collision situation is confirmed, a control system adjusts the input to the ACM via a feedback mechanism which compares the current actual buckling eigenvalue, denoted λ_c, relating to the buckling load, with the most recently updated desired eigenvalue λ_d, from a pre-calculated multi-dimensional look-up table (MDLT) (Trollope, et al., 2014). This update corresponds to the most recently estimated vehicle masses and estimated collision velocity. Mass and velocity information is routinely generated, hence available on each host vehicle to transmit via V2V, which allows each host to transfer to each partner. However not all vehicles are equipped with V2V so there is a need to estimate the trajectories based on a model with use being made of a Kalman filter (KF) approach, see Section 3.2.

3.1 Multi-dimensional look-up table using fuzzy logic

In the case of a full frontal collision use is made of a pre-calculated MDLT (Fig. 2) relating to the different collision scenarios. These different scenarios give rise to different collision energies ΔE (delta energy). As is evident from (2) the value of ΔE is effected by the mass of the vehicles and velocity of the collision, where the distribution of ΔE is based on the vehicle mass ratios, as defined in (4) and (5). Therefore, knowing ΔE, the desired buckling point for each VBS is determined based on the desired energy absorption distribution between the colliding vehicles. Thus the smallest positive eigenvalues λ_a and λ_b may be determined for the host Vehicle A and partner Vehicle B, respectively.

The 'ideal' apportionment of collision energy for the host Vehicle A (Fig. 3) and partner Vehicle B (Fig. 4) is given for the different mass values of each vehicle. Thus the case to support the use of ABC has been presented, for without the use of ABC, the graphs are effectively reversed i.e. Vehicle A (Fig. 4) and Vehicle B (Fig. 3).

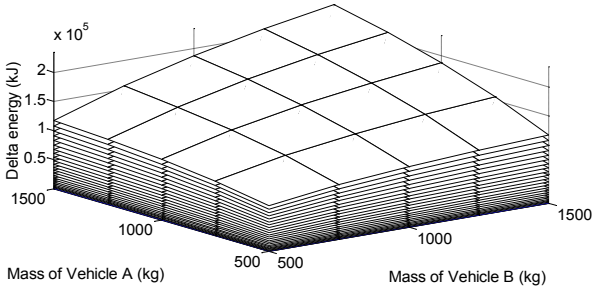

Fig. 2. Delta Energy of a Two Vehicle Frontal Collision

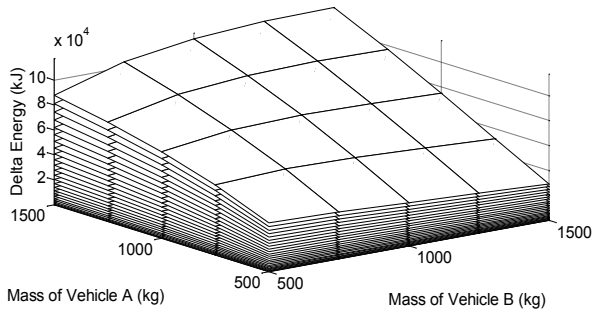

Fig. 3. Delta Energy distributed to Vehicle A (ideal)

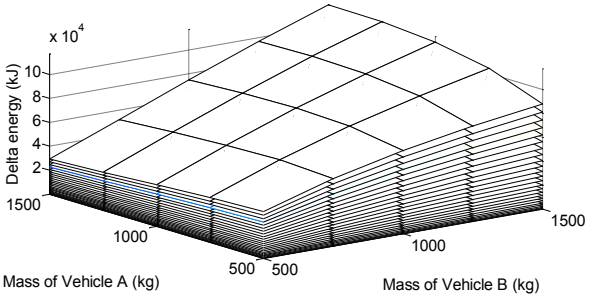

Fig. 4. Delta Energy distributed to Vehicle B (ideal)

3.*2 Kalman filter approach*

A fine-tuned adaptive update is achieved by making use of a KF approach, which supplies updated vehicle data to the ABC system. During the time period between collision anticipation and prior to the collision taking place, the KF is active to refine the eigenvalues as updated estimates of the collision velocity become available. At a point Δt prior to the collision further refinement ceases and the VBS mechanical properties are adjusted accordingly to achieve the desired collision energy distribution.

4. MODEL OF VEHICLE BODY STRUCTURE

This Section develops a general lumped parameter mass, spring and damper model for two colliding vehicles.

4.1 Longitudinal members

As highlighted in Section 1, the VBS is made up of crumple zones and a passenger compartment. The crumple zones are located at the front and rear of the vehicle, and comprise of load bearing longitudinal members. In this paper, the focus will be on developing frontal impact models, therefore, only the front ends of two colliding vehicles are considered. Whilst the model developed here is capable of handling offset frontal collisions, having independent actively controlled left and right longitudinal members, the model in this work is utilised for full frontal collisions only, hence the left and right mechanical properties are lumped together into a single spring and damper configuration. However, the full equations capable of differentiating between the modulation of the left and right sides are developed here for completeness.

4.2 Free body considerations

A full-frontal impact model for two vehicles, whose masses are denoted m_a and m_b is modelled using springs and dampers with lumped masses to represent the components. The two bumper assemblies, denoted m_c, are modelled as one lumped mass (Fig. 5), since they remain together after impact (perfectly plastic impact) and have the same velocity and displacement. In this case, the model has three degrees of freedom, with corresponding displacements x_1, x_2 and x_3. The two vehicles have initial velocities, V_a and V_b, with $V_a = 12m/s$ and $V_b = 0m/s$. The stiffness elements shown as springs are denoted k_{ij}, these being the plastic deformation parts representing the longitudinal members (Fig. 5). The damping coefficients are represented as d_{ij}, where in both cases, the subscripts i represent Vehicle A or B and j represents the left or right longitudinal member.

From the free body diagram (Fig. 5) of the combined vehicles, mass spring and damper elements, the differential equations of motion using Newton's third law to sum the forces to zero are derived as follows:

$$M_n\ddot{x} + D_n\dot{x} + K_n x = F \tag{6}$$

with x, $\dot{x}$ and $\ddot{x}$ being the nodal displacements, velocities and accelerations, respectively, and F being the vector containing external forces. Considering (6) the following equations can be developed for Vehicles A and B:

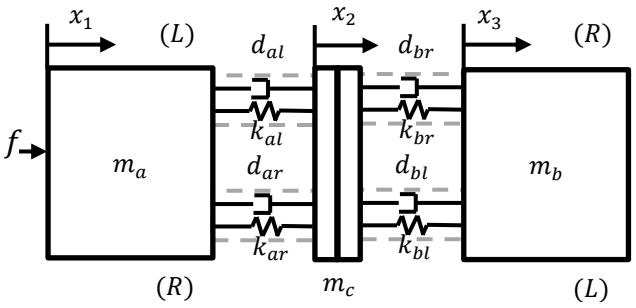

Fig. 5. Three mass, spring and damper system of two vehicles

$$m_a\ddot{x}_1 + k_{al}(x_1 - x_2) + d_{al}(\dot{x}_1 - \dot{x}_2) = f \tag{7}$$

$$m_c\ddot{x}_2 + k_{ar}(2x_2 - x_1 - x_3) + d_{ar}(2\dot{x}_2 - \dot{x}_1 - \dot{x}_3) = 0 \tag{8}$$

$$m_b\ddot{x}_3 + k_{br}(x_3 - x_2) + d_{br}(\dot{x}_3 - \dot{x}_2) = 0 \tag{9}$$

$$m_a\ddot{x}_1 + k_{ar}(x_1 - x_2) + d_{ar}(\dot{x}_1 - \dot{x}_2) = f \tag{10}$$

$$m_c\ddot{x}_2 + k_{br}(2x_2 - x_1 - x_3) + d_{br}(2\dot{x}_2 - \dot{x}_1 - \dot{x}_3) = 0 \tag{11}$$

$$m_b\ddot{x}_3 + k_{bl}(x_3 - x_2) + d_{bl}(\dot{x}_3 - \dot{x}_2) = 0 \tag{12}$$

Expressing the above equations in the matrix form (6), having the mass matrix $M_n = diag(m_a, m_b, m_c)$ the stiffness and damping matrices are given by:

$$K_n = \begin{bmatrix} k_{al} & -k_{al} & 0 \\ -k_{ar} & 2k_{ar} & -k_{ar} \\ 0 & -k_{br} & k_{br} \end{bmatrix} + \begin{bmatrix} k_{ar} & -k_{ar} & 0 \\ -k_{br} & 2k_{br} & -k_{br} \\ 0 & -k_{bl} & k_{bl} \end{bmatrix} \tag{13}$$

$$D_n = \begin{bmatrix} d_{al} & -d_{al} & 0 \\ -d_{ar} & 2d_{ar} & -d_{ar} \\ 0 & -d_{br} & d_{br} \end{bmatrix} + \begin{bmatrix} d_{ar} & -d_{ar} & 0 \\ -d_{br} & 2d_{br} & -d_{br} \\ 0 & -d_{bl} & d_{bl} \end{bmatrix} \tag{14}$$

In practice the equations are normalised such that: $M_n = I_3$.

5. MODELLING CHARACTERISTICS OF A CRASH

Before the event of a collision, the vehicle masses are assumed to be estimated along with the collision velocity. During a collision the mass remains constant. However, the stiffness and damping will be dependent on the displacement (deformation) and velocity values during the collision.

A typical force versus deformation frontal collision characteristic curve (Fig 6.) initially indicates that 0 to 85mm represents the collapse of the vehicles bumper structure, where low forces are experienced. Between approximately 85 and 470mm the plot corresponds to buckling, with the structure being in its plastic state, whereas beyond 470mm towards the end of deformation, the structure returns to an elastic state, with the material deformation returning from approximately 620 to 520mm. Consequently, the area under the curve, between 85 and 470mm represents the work done, corresponding to ΔE, during deformation.

When a VBS is designed to absorb more energy, the structures are encouraged to collapse earlier so that energy absorption commences at a lower initial buckling load, related to the buckling eigenvalue. Conversely, when a VBS is stiffened the initial buckling load is increased to resist the onset of buckling, hence energy absorption.

The initial modelling of the crash characteristic assumes a linear relationship between force, denoted f, and displacement, in the region between the dotted lines (Fig. 6).

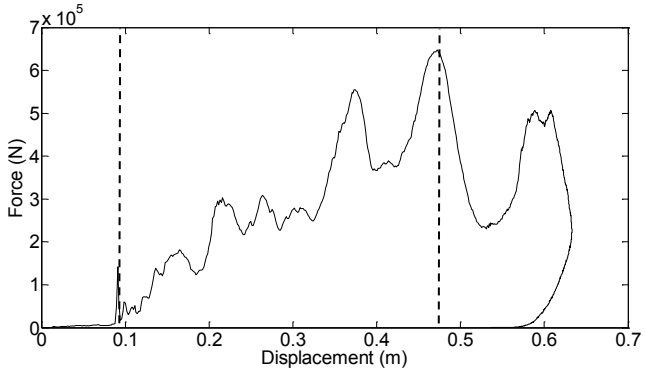

Fig. 6. Force – displacement crash characteristic

5.1 Linear approximation

A linear approximation is obtained using a least squares fitting technique such that the characteristic is found to be

$$(F_s)_{ij}(\delta_{ij}) = f_p + \alpha_{ij}\delta_{ij} \quad (15)$$

where f_p is the fixed force at a displacement of approximately 85mm and α is the average gradient (Fig. 7).

5.2 Piece-wise linear approximation

A two-section piecewise linear approximation provides an improvement whereby between approximately 85mm and a point δ^*_{ij}, a linear characteristic is obtained and from the point δ^*_{ij} to approximately 470mm another linear characteristic is obtained (Fig. 8).

$$(F_s)_{ij}(\delta_{ij}) = f_p + \alpha_{1_{ij}}.\delta_{ij} \qquad \delta_{ij} \le \delta^*_{ij} \quad (16)$$

$$(F_s)_{ij}(\delta_{ij}) = f_p + \alpha_{1_{ij}}\,\delta^*_{ij} + \alpha_{2_{ij}}\,(\delta_{ij} - \delta^*_{ij}) \quad (17)$$

$$\delta_{ij} \le \delta^*_{ij}$$

5.3 Bilinear approximation

Bilinear models have been successfully applied to various practical applications to provide a nonlinear approximation. Essentially, the model takes the form:

$$(F_s)_{ij}(\delta_{ij}) = f_p + \Omega_{ij}\delta_{ij} + \Upsilon_{ij}\delta_{ij}(F_s)_{ij}(\delta_{ij}) \quad (18)$$

which may be further simplified to

$$(F_s)_{ij}(\delta_{ij}) = (f_p + \Omega_{ij}\delta_{ij})/(1 - \Upsilon_{ij}\delta_{ij}) \quad (19)$$

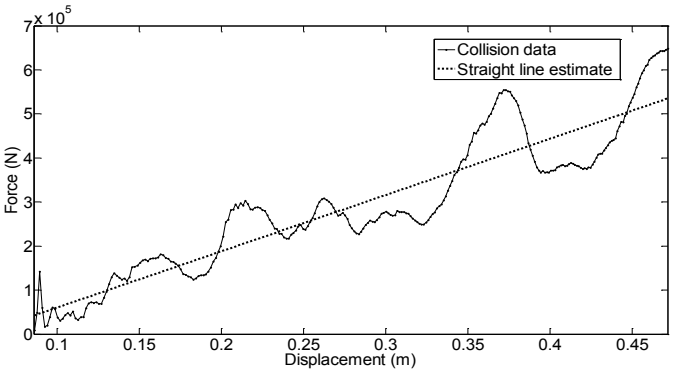

Fig. 7. Force – displacement linear characteristic

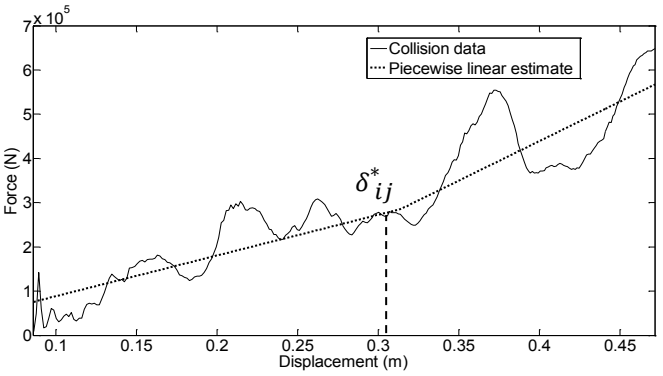

Fig. 8. Force – displacement piecewise linear characteristic

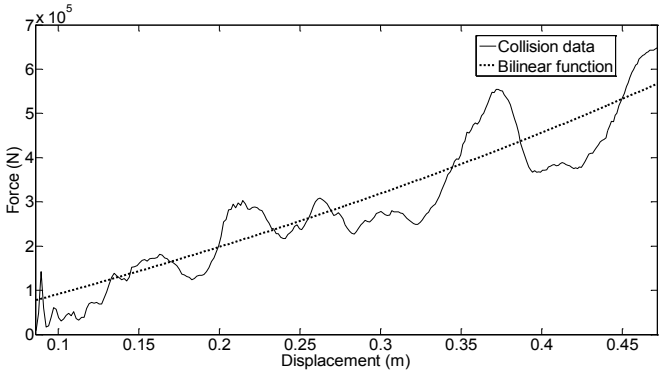

Fig. 9. Force – displacement bilinear characteristic

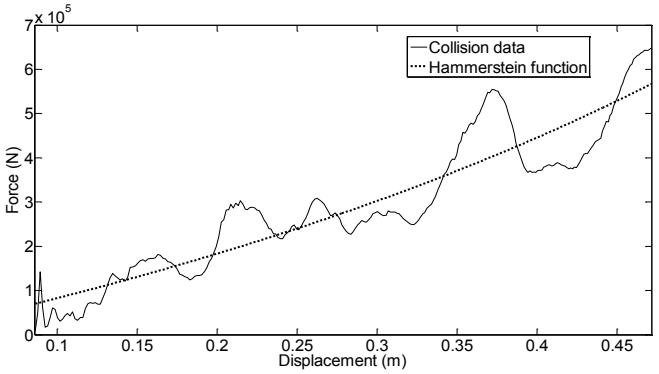

Fig. 10. Force – displacement Hammerstein-bilinear characteristic

The approach (Fig. 9) offers flexibility to tune the characteristics via Ω_{ij} and Υ_{ij}.

5.4 Hammerstein-bilinear approximation

To allow greater flexibility (Fig. 10) in the modelling of the characteristic, additional Hammerstein terms can be included. An approach investigated here introduces a squared term into the model, such that

$$F(s)_{ij}(\delta_{ij}) = f_p + \bar{\Omega}_{ij}\delta_{ij} + \bar{\Upsilon}_{ij}\delta_{ij}(F(s))_{ij}(\delta_{ij}) + X\delta_{ij}^2 \quad (20)$$

$$F(s)_{ij}(\delta_{ij}) = (f_p + \bar{\Omega}_{ij}\delta_{ij} + \bar{\Upsilon}_{ij}\delta_{ij}^2)/(1 - \Upsilon_{ij}\delta_{ij}) \quad (21)$$

where the '¯'notation indicates that, e.g. Ω and $\bar{\Omega}$, are different quantities.

5.6 Comparing accuracy of results

The effectiveness of four modelling approaches are compared using as a metric the mean sum of squares of errors i.e. $\sum \frac{e^2}{N}$ normalised to unity with the linear baseline model.

Table 1. Summary of results

Method	Normalised squared errors
Linear	1
Piecewise linear	0.9971
Bilinear	0.9919
Hammerstein bilinear	0.9921

6. SIMULATION STUDY

The models developed in Sections 4 and 5 are simulated to demonstrate the effect and benefits of varying the stiffness of the VBS longitudinal members.

6.1 Data used for numerical simulation

The following data is used: mass of Vehicle B is fixed at 500kg, mass of Vehicle A ranges from m_b to $4m_b$ and the mass of the combined bumper assembly is 50kg. The force-displacement characteristic (18-19) of the bilinear model is adopted (Fig. 9), due to its marginally slightly better fit.

6.2 Demonstration of ABC

The effect of collisions with vehicles of dissimilar mass is demonstrated via comparison of the case of use of ABC and the case of not using ABC.

The results from not using ABC (upper-plot Fig. 11) show the increasing deformation of Vehicle B. The concept and effectiveness of ABC is now demonstrated by increasing the stiffness of the smaller vehicle; the aim being to reduce the aggressivity of the collision. It can be seen (lower-plot Fig. 11) that, in the case of use of ABC, the deformation of the smaller vehicle is reduced, hence alleviating the compatibility problem, with the larger vehicle absorbing more energy.

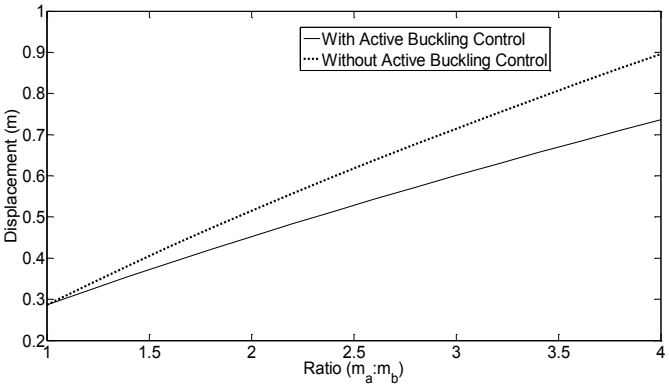

Fig. 11. Displacement-mass ratio case of with/without ABC

7. CONCLUSIONS

This paper has introduced the concept of active buckling control applied to lightweight vehicles to alleviate the compatibility problem, thereby reducing the aggressivity (imbalance of energy absorption) when two vehicles of dissimilar mass collide. A simulation study has demonstrated the effectiveness of the approach, highlighting the principles of active control of vehicle body structures. It has been shown that energy absorption can be apportioned more appropriately via the proposed actively controlled approach. BC

8. FURTHER WORK

Further work involves the decoupling of the eigenvalue assignment problem, making use of a modal control formulation. Realisation of active buckling control together with an investigation of the potential of piezoelectric and shape memory alloy materials to achieve the desired outcomes is to be undertaken, as well as optimising the material locations within the vehicle body structures.

REFERENCES

Ellis, M. (2011). Material Selection & Application for Future Low Carbon Vehicles, Aluminium Federation Automotive Conference.

European NCAP. (2013). European New Car Assessment Programme Frontal Impact Testing Protocol. Version 6.0.1, July.

Thatcham Insight. (2012). Automotive Insight for Members. No.3, November.

Trollope, J.E., and Burnham, K.J. (2013a). Active Buckling Control. (UK Patent Pending GB1320489.6).

Trollope, J.E., and Burnham, K.J. (2013b) Active Buckling Control for Future Lightweight Vehicle Body Structures. *Measurement and Control*. 46 (10), 315-320.

Trollope, J.E., Pozniak-Koszalka, I., Koszalka, L., and Burnham, K.J. (2014). Active Buckling Control for Vehicle Body Structures: A Fuzzy Logic Approach for Collision Energy Distribution, Control 2014, UKACC 10th International Conference on Control, Loughborough, UK, July.